

# Grootfonteinite, $\text{Pb}_3\text{O}(\text{CO}_3)_2$ , a new mineral species from the Kombat Mine, Namibia, merotypically related to hydrocerussite

OLEG I. SIIDRA<sup>1,2,\*</sup>, ERIK JONSSON<sup>3,4</sup>, NIKITA V. CHUKANOV<sup>5</sup>, DIANA O. NEKRASOVA<sup>1</sup>, IGOR V. PEKOV<sup>6</sup>, WULF DEPMEIER<sup>7</sup>, YURY S. POLEKHOVSKY<sup>8</sup> and VASILIIY O. YAPASKURT<sup>6</sup>

<sup>1</sup> Department of Crystallography, St. Petersburg State University, University emb. 7/9, 199034 St. Petersburg, Russia

\*Corresponding author, e-mail: [o.siidra@spbu.ru](mailto:o.siidra@spbu.ru)

<sup>2</sup> Kola Science Center, Russian Academy of Sciences, Apatity, Murmansk Region, 184209, Russia

<sup>3</sup> Geological Survey of Sweden, Department of Mineral Resources, Box 670, 75128 Uppsala, Sweden

<sup>4</sup> Department of Earth Sciences, Uppsala University, 75236 Uppsala, Sweden

<sup>5</sup> Institute of Problems of Chemical Physics, Chernogolovka, Moscow region, 142432, Russia

<sup>6</sup> Faculty of Geology, Moscow State University, Vorobievsky Gory, 119991, Moscow, Russia

<sup>7</sup> Institut für Geowissenschaften der Universität Kiel, Olshausenstr. 40, 24098 Kiel, Germany

<sup>8</sup> Department of Mineral Deposits, St. Petersburg State University, University emb. 7/9, 199034 St. Petersburg, Russia

**Abstract:** Grootfonteinite,  $\text{Pb}_3\text{O}(\text{CO}_3)_2$ , is a new Pb oxycarbonate found in a mineralogically complex, banded assemblage from the Mn (-Fe) oxide ore unit of the Kombat mine. Grootfonteinite is named after the locality in the Grootfontein district. The mineral forms platy grains up to 1 mm across and up to 0.2 mm thick included in and intergrown with massive cerussite. Grootfonteinite is colourless, with white streak and adamantine lustre. It is brittle with perfect cleavage on (001). The density calculated using the empirical formula  $\text{H}_{0.345}\text{Na}_{0.275}\text{Ca}_{0.045}\text{Pb}_{2.645}\text{C}_2\text{O}_7$  is  $6.856 \text{ g} \cdot \text{cm}^{-3}$ . The strongest five reflections in the X-ray powder-diffraction pattern [ $d$  in Å)-(Intensity)-(hkl)] are: 4.586-25-0 1 0, 3.244-100-0 1 3, 2.652-30-1 1 0, 2.294-21-0 2 0, 2.053-39-0 2 3. Grootfonteinite crystallizes in space group  $P6_3/mmc$  (No. 194),  $a = 5.303(1)$ ,  $c = 13.770(3)$  Å,  $V = 335.3(1)$  Å<sup>3</sup>,  $Z = 2$ . The crystal structure of grootfonteinite is formed by layered blocks which consist of sheets with composition  $[\text{PbCO}_3]$  and (ideally)  $[\text{PbO}]$ , the stacking of which can be described as ...-[ $\text{PbCO}_3$ ]-[ $\text{PbO}$ ]-[ $\text{PbCO}_3$ ]-... The composition of the resulting electroneutral 2D block is  $\{[\text{Pb}_2(\text{CO}_3)_2][(\text{Pb}_{0.7}\text{Na}_{0.3})(\text{O}_{0.7}(\text{OH})_{0.3})]\}^0$ . The stereochemically active  $6s^2$  lone electron pairs of the two Pb atoms are located in between the blocks, resembling the classical case of the structure of litharge. Grootfonteinite is structurally related to hydrocerussite, abellaite, and plumbonacrite. A characteristic structural feature of all these minerals is the presence of  $[\text{PbCO}_3]^0$  sheets in the upper and lower parts of invariably electroneutral 2D blocks, the middle part being variable. The topology of 2D blocks in the crystal structure of grootfonteinite can be considered as intermediate between those of abellaite and hydrocerussite. These three minerals can be considered to form a merotype family. Other members of this family can be hypothesized which differ in the nature of the interleaved sheets.

**Key-words:** grootfonteinite; carbonate; lead; hydrocerussite; abellaite; layered structure; new mineral; Kombat mine.

## 1. Introduction

Minerals containing heavy metals and which form under near-ambient conditions have attracted considerable attention in recent years, not least because of their importance for environmental issues. Such minerals are important in the context of the mobilization and transport of Pb from mine and mill tailings into the biosphere, as well as of its sequestration in order to prevent such distribution. Knowledge of the crystal chemistry of these minerals is important for the understanding of transport and re-deposition of Pb during weathering. Among these minerals, particularly Pb carbonates and hydroxycar-

bonates are known as the main phases formed during lead corrosion. In modern industry they are also used as polymer stabilizers (Grossman & Lutz, 2000). The formation of Pb hydroxycarbonates is also important for the performance of lead acid batteries, because their presence in and on battery plates reduces the acid permeability within the  $\text{PbO}_2$  network, and increases the resistivity of the electrolyte. Furthermore, the formation, presence and characterisation of hydrocerussite-related phases have various implications for archeology and technical analysis of artwork (Gonzalez *et al.*, 2016; Welcomme *et al.*, 2006; Scott *et al.*, 2003). To date, three Pb hydroxycarbonate minerals are known, viz. hydrocerussite  $\text{Pb}_3(\text{OH})_2(\text{CO}_3)_2$

(e.g. Keller, 1977), plumbonacrite  $\text{Pb}_5\text{O}(\text{OH})_2(\text{CO}_3)_3$  (Rumsey *et al.*, 2012) and abellaite  $\text{NaPb}_2(\text{OH})(\text{CO}_3)_2$  (Ibáñez-Insa *et al.*, 2017).

The new Pb oxycarbonate mineral grootfonteinite was discovered in a sample that was collected during underground mining already in the mid-1980s to early 1990s in the Kombat mine, Grootfontein district, Otjozondjupa region, northern Namibia (WGS 84 coordinates  $19^\circ 46' 60'' \text{S}$ ,  $18^\circ 1' 0'' \text{E}$ ). Grootfonteinite (Cyrillic: хрутфонтейнит) is named for the locality in the Grootfontein district. The mineral and its name have been approved by the Commission on New Minerals, Nomenclature and Classification of the International Mineralogical Association (2015-051). The type material is deposited in the collections of the Swedish Museum of Natural History (Stockholm, Sweden), under the catalogue number 20080176.

## 2. Locality and occurrence

Grootfonteinite occurs in a mineralogically complex, banded assemblage from the Mn(-Fe) oxide ore unit of the Kombat mine. Based on the mineral assemblage, we find it likely that it originates from the Asis West sector of the mine, the source of several previous mineral discoveries (e.g. Peacor *et al.*, 1988a, b; Sarp & Peacor, 1989; Criddle *et al.*, 1990; Hawthorne *et al.*, 2013). Textural and paragenetic observations suggest that the mineral may have formed as a consequence of regional metamorphism (Damaran, e.g. Innes & Chaplin, 1986) of a primary, Pb-Mn-(As-Ba)-rich, chemically heterogeneous, volcanic-hydrothermal assemblage. This and several related assemblages from the Mn(-Fe) oxide ore unit at Kombat bear remarkable similarity to some assemblages from the Långban mine, Sweden (Nysten *et al.*, 1999), and both occurrences may share several common aspects of their general process of formation. Grootfonteinite occurs in association with jacobsonite, cerussite, dolomite, clinocllore, hausmannite, melanotekite, sahlinitite, rhodochrosite, and baryte.

## 3. Experimental procedure

### 3.1. Physical properties and optical data

Grootfonteinite forms platy grains up to 1 mm across and up to 0.2 mm thick included in, and intergrown with, massive cerussite (Fig. 1), and as larger, strongly poikilitic, platy aggregates up to a diameter of several mm in one portion of the studied material. Grootfonteinite is colourless, with white streak and adamantine lustre. It is brittle with a perfect cleavage on (001). Parting was not observed, and its fracture is uneven across the cleavage planes. The density could not be measured due to lack of sufficient material and the non-availability of heavy liquids with densities between 6 and  $7 \text{ g} \cdot \text{cm}^{-3}$ . The calculated density using the empirical formula derived from the analytical data given in Table 1 is  $6.856 \text{ g} \cdot \text{cm}^{-3}$ . Grootfonteinite has a Vickers Hardness

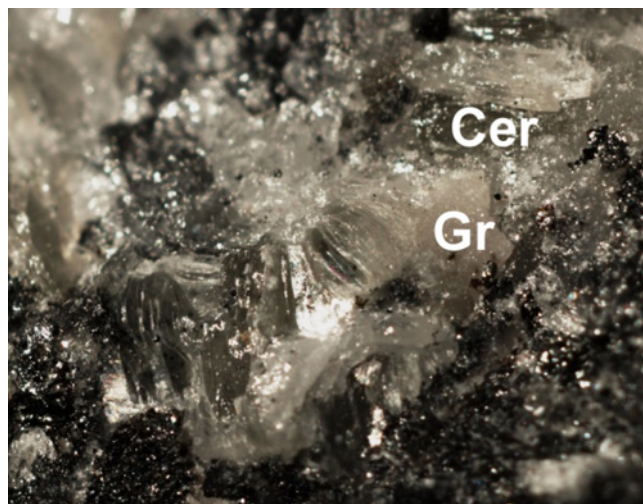


Fig. 1. Highly lustrous, intergrown platelets of grootfonteinite (Gr = light) in massive Ca-bearing cerussite (Cer = dark), associated with black Mn-Fe oxides. Field of view 5 mm.

Table 1. Chemical composition of grootfonteinite (average of 10 spot analyses, with standard deviation, S. D.).

| Constituent | wt%    | Range       | S. D. | Probe standard    |
|-------------|--------|-------------|-------|-------------------|
| Na          | 0.92   | 0.88–0.95   | 0.02  | lorenzenite       |
| Ca          | 0.26   | 0.23–0.29   | 0.02  | wollastonite      |
| Pb          | 79.66  | 79.40–80.09 | 0.24  | PbTe              |
| O           | 16.28  | 15.70–17.02 | 0.38  | NdPO <sub>4</sub> |
| C (calc.)   | 3.49*  |             |       |                   |
| H (calc.)   | 0.05** |             |       |                   |
| Total       | 100.66 |             |       |                   |

\* Calculated by stoichiometry, for 2C *apfu*;

\*\* calculated by charge balance. Contents of other elements with atomic numbers higher than carbon are below detection limits.

Number ( $\text{VHN}_{20}$ ) of  $55.3 \text{ kg} \cdot \text{mm}^{-2}$  ( $n=5$ , range  $48.7\text{--}66.1 \text{ kg} \cdot \text{mm}^{-2}$ ), which approximately corresponds to a Mohs' hardness of 2.

Despite the transparency of grootfonteinite, its optical properties had to be investigated in reflected light, because of the high values of refractive indices. Reflectance measurements were made using a SiC standard (Zeiss, No. 545) in air in the range 400–700 nm (Table 2). In reflected light, grootfonteinite is grey. It is non-pleochroic, with white internal reflections and a very weak bireflectance. The measured anisotropy is  $\Delta R_{589} = 2.1\%$ ; under the optical microscope, the relatively weak anisotropy is masked by abundant internal reflections.

### 3.2. Chemical composition

The chemical composition of grootfonteinite (Table 1) was determined using a Jeol JSM-6480LV scanning electron microscope equipped with an INCA-Wave 500 wavelength-dispersive spectrometer (Laboratory of Analytical

Table 2. Reflectance values of an unoriented section free of internal reflections on a measured area of  $20 \times 20 \mu\text{m}$  (SiC standard, measured in air) for grootfonteinite.

| $\lambda$ , nm | $R_{\text{max}}$ , % | $R_{\text{min}}$ , % | $\lambda$ , nm | $R_{\text{max}}$ , % | $R_{\text{min}}$ , % |
|----------------|----------------------|----------------------|----------------|----------------------|----------------------|
| 400            | 13.9                 | 11.7                 | 560            | 12.6                 | 10.4                 |
| 420            | 13.6                 | 11.4                 | 580            | 12.5                 | 10.4                 |
| 440            | 13.3                 | 11.1                 | <b>589</b>     | <b>12.5</b>          | <b>10.3</b>          |
| 460            | 13.1                 | 10.9                 | 600            | 12.4                 | 10.3                 |
| <b>470</b>     | <b>13.0</b>          | <b>10.8</b>          | 620            | 12.4                 | 10.3                 |
| 480            | 12.9                 | 10.7                 | 640            | 12.3                 | 10.2                 |
| 500            | 12.8                 | 10.6                 | <b>650</b>     | <b>12.3</b>          | <b>10.2</b>          |
| 520            | 12.7                 | 10.5                 | 660            | 12.2                 | 10.2                 |
| 540            | 12.6                 | 10.5                 | 680            | 12.2                 | 10.2                 |
| <b>546</b>     | <b>12.6</b>          | <b>10.5</b>          | 700            | 12.1                 | 10.2                 |

Techniques of High Spatial Resolution, Dept. of Petrology, Moscow State University), with an acceleration voltage of 20 kV and a beam current of 20 nA; the electron beam was rastered within a  $5 \mu\text{m} \times 5 \mu\text{m}$  area to minimize damage to the sample. The contents of elements with atomic numbers higher than that of carbon, including oxygen, were measured directly while the C and H contents had to be calculated – see footnote in Table 1.

The empirical formula of grootfonteinite, calculated on the basis of 7 O and 2C *apfu* (atoms per formula unit), is  $\text{H}_{0.345}\text{Na}_{0.275}\text{Ca}_{0.045}\text{Pb}_{2.645}\text{C}_2\text{O}_7$ . The simplified formula is  $\text{Pb}_3\text{O}(\text{CO}_3)_2$ , which requires (in wt%) Pb 82.05, C 3.17, O 14.78, total 100.00 wt%.

### 3.3. Infrared spectroscopy

In order to obtain IR absorption spectra, powdered samples were mixed with anhydrous KBr, pelletized, and analyzed using an ALPHA FTIR spectrometer (Bruker Optics) with a resolution of  $4 \text{cm}^{-1}$ ; 16 scans were taken. The IR spectrum of an analogously prepared pellet of pure KBr served as a reference.

The IR spectrum of grootfonteinite is rather similar to those of the related minerals hydrocerussite and plumbonacrite (Fig. 2). Wavenumbers of absorption bands in the IR spectrum of grootfonteinite and their assignments are ( $\text{cm}^{-1}$ ; s – strong band, w – weak band, sh – shoulder): 3470 w, 3386 w (O–H-stretching vibrations); 1738 (overtone of in-plane bending vibrations of  $\text{CO}_3^{2-}$  anions); 1418 s, 1380 sh (asymmetric C–O-stretching vibrations of  $\text{CO}_3^{2-}$  anions); 1200 (combination mode involving Pb–O-stretching and O–C–O bending vibrations); 1046 (symmetric C–O-stretching vibrations of  $\text{CO}_3^{2-}$  anions); 837 (out-of-plane bending vibrations of  $\text{CO}_3^{2-}$  anions); 685 sh, 680 s (in-plane bending vibrations of  $\text{CO}_3^{2-}$  anions); 480 (Pb–O-stretching vibrations).

Grootfonteinite reveals several times weaker bands of O–H-stretching vibrations in the range of 3300–3600  $\text{cm}^{-1}$  as compared with hydrocerussite and plumbonacrite. The position of the strongest band of asymmetric C–O-stretching vibrations of  $\text{CO}_3^{2-}$  anions in the IR spectrum of grootfonteinite (1418  $\text{cm}^{-1}$ ) is intermediate

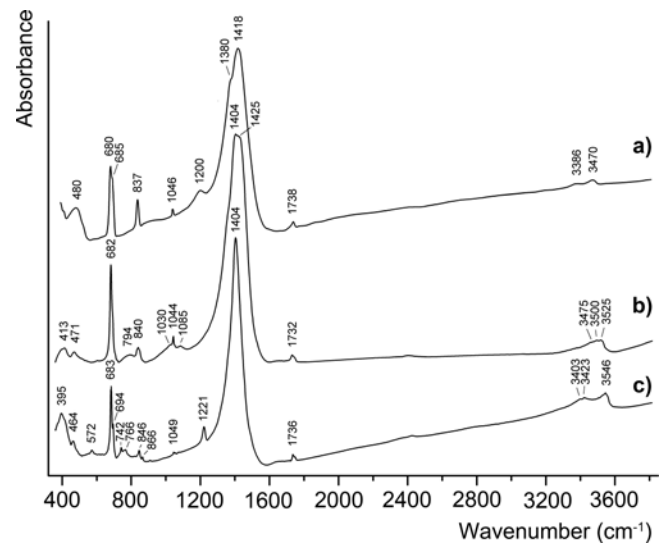


Fig. 2. IR spectra of grootfonteinite (a), hydrocerussite from Legrain, Lavrion, Greece (b), and plumbonacrite from Långban, Sweden (c).

between the positions of corresponding bands of the synthetic compound  $\text{NaPb}_2(\text{OH})(\text{CO}_3)_2$  (1435  $\text{cm}^{-1}$ , see Brooker *et al.*, 1983), and hydrocerussite and plumbonacrite (1404  $\text{cm}^{-1}$  for both).

The presence of a weak band of symmetric C–O-stretching vibrations of  $\text{CO}_3^{2-}$  anions (at 1046  $\text{cm}^{-1}$ ) in the IR spectrum of grootfonteinite reflects a local asymmetry of the  $\text{CO}_3^{2-}$  groups due to partial substitution of Pb by Na in the Pb(1) site (see below).

### 3.4. X-ray crystallography

Preliminary X-ray powder diffraction data revealed that grootfonteinite is closely associated with cerussite and forms intimate intergrowths with it. Thus it was decided to hand-pick 10 homogenous lamellar crystals of grootfonteinite under the microscope. These were first checked on a single-crystal X-ray diffractometer, and subsequently crushed and mounted in an epoxy ball with  $R \sim 0.5 \text{mm}$  on a glass fibre. X-ray powder diffraction data were collected with  $\text{CoK}\alpha$  radiation by means of a Rigaku RAXIS Rapid II single-crystal diffractometer equipped with a cylindrical image plate detector using Debye-Scherrer geometry (with  $d = 127.4 \text{mm}$ ). The data are given in Table 3. The lattice parameters refined in the hexagonal unit cell, are:  $a = 5.300(2)$ ,  $c = 13.761(2) \text{\AA}$ ,  $V = 334.88(23) \text{\AA}^3$ ,  $Z = 2$ .

A very thin lamellar crystal ( $0.12 \times 0.12 \times 0.005 \text{mm}^3$ ) was mounted on a Bruker APEX II DUO X-ray diffractometer with a micro-focus X-ray tube operated with  $\text{MoK}\alpha$  radiation at 50 kV and 40 mA. The data were integrated and corrected for absorption using a multi-scan model and the Bruker programs *APEX* and *SADABS* (Bruker-AXS, 2014). More than a hemisphere of X-ray diffraction data was collected for each crystal with frame widths of  $0.3^\circ$  in  $\omega$ , and 55 s counting time for each frame. The observed reflection conditions of grootfonteinite were consistent with space groups  $P31c$ ,  $P-31c$ ,  $P6_3mc$  and

Table 3. Powder X-ray diffraction data for grootfonteinite (space group  $P6_3/mmc$ ). The six strongest diffraction lines are in bold.

| $hkl$ | $d_{\text{calc.}} \text{ \AA}$ | $I_{\text{calc.}} \%$ | $d_{\text{meas.}} \text{ \AA}$ | $I_{\text{meas.}} \%$ |
|-------|--------------------------------|-----------------------|--------------------------------|-----------------------|
| 002   | 6.885                          | 1                     |                                |                       |
| 100   | 4.592                          | 29                    | <b>4.586</b>                   | <b>25</b>             |
| 101   | 4.357                          | 8                     | 4.353                          | 9                     |
| 004   | 3.443                          | 6                     | 3.441                          | 8                     |
| 103   | 3.247                          | 100                   | <b>3.244</b>                   | <b>100</b>            |
|       |                                |                       | <b>2.652</b>                   | <b>30</b>             |
| 110   | 2.651                          | 41                    | <b>2.627</b>                   | <b>12</b>             |
| 112   | 2.474                          | 1                     | 2.474                          | 2                     |
| 200   | 2.296                          | 8                     | <b>2.294</b>                   | <b>21</b>             |
| 006   | 2.295                          | 10                    |                                |                       |
| 201   | 2.265                          | 6                     | 2.267                          | 5                     |
| 202   | 2.178                          | 1                     |                                |                       |
| 114   | 2.101                          | 2                     | 2.101                          | 3                     |
| 203   | 2.054                          | 29                    | <b>2.053</b>                   | <b>39</b>             |
| 106   | 2.053                          | 8                     |                                |                       |

$P6_3/mmc$ . The structure was solved using direct methods (SHELX, Sheldrick, 2015) in space group  $P31c$ . Refinements in this or the other space groups of lower symmetry were not satisfactory, either because the light atoms (C, O) could not be refined anisotropically or unrealistic bond lengths resulted. Therefore the obtained structure model was transformed into space group  $P6_3/mmc$  using the ADDSYM algorithm incorporated in the PLATON program package (Le Page, 1987; Spek, 2003). This model was successfully refined using the SHELX software package (Sheldrick, 2015) converging to  $R_1=0.052$  (Table 4). It should be noted that the positional disorder of the Pb2 atom discussed further below was observed in all tested space groups and should therefore be considered real. The unit-cell parameters (Table 5) indicate that the crystal structure of grootfonteinite is closely related to the previously reported synthetic compound  $\text{NaPb}_2(\text{CO}_3)_2(\text{OH})$  (Krivovichev & Burns, 2000a; Belokoneva *et al.*, 2002), as well as to its recently described natural analogue abellaite  $\text{NaPb}_2(\text{CO}_3)_2(\text{OH})$  (Ibáñez-Insa *et al.*, 2017). Note, however, that the  $c$  parameter of grootfonteinite exceeds those of abellaite and synthetic  $\text{NaPb}_2(\text{CO}_3)_2(\text{OH})$  by  $\sim 0.3 \text{ \AA}$ . The  $a$  parameter is nearly identical to that of hydrocerussite (Table 5). We have recently determined the crystal structure of hydrocerussite from Merehead quarry, England by single-crystal X-ray diffraction and a detailed description will be reported in the near future. This structural model of hydrocerussite obtained from a twinned crystal is very similar to that obtained by X-ray powder diffraction published in Martinetto *et al.* (2002). Krivovichev & Burns (2000a) refined the crystal structure of synthetic  $\text{NaPb}_2(\text{CO}_3)_2(\text{OH})$  in  $P6_3mc$ . For the same compound a different model in space group  $P31c$  was published later by Belokoneva *et al.* (2002). From our present refinement of the crystal structure of grootfonteinite and the very good match of the corresponding diffraction patterns we suppose that  $\text{NaPb}_2(\text{CO}_3)_2(\text{OH})$  is most likely also centrosymmetric, *i.e.* crystallizes in space group

Table 4. Crystallographic data and structure refinement details for grootfonteinite.

| Crystal data                                     |  |
|--|--|
| Crystal system                                   | hexagonal  |
| Space group                                      | $P6_3/mmc$   |
| Unit cell dimensions                             |  |
| $a$ (Å)  | 5.303(1)   |
| $c$ (Å)  | 13.770(3)  |
| Unit-cell volume (Å <sup>3</sup> )               | 335.3(1)   |
| $Z$  | 2  |
| Crystal size (mm)                                | $0.12 \times 0.12 \times 0.005$                          |
| Data collection                                  |  |
| Temperature (K)                                  | 296(2)   |
| Radiation, wavelength (Å)                        | MoK $\alpha$ , 0.71073                                   |
| $\theta$ range (°)                               | 2.958–27.852   |
| $h, k, l$ ranges                                 | $-6 \rightarrow 6, -6 \rightarrow 6, -16 \rightarrow 18$ |
| Total reflections collected                      | 3440   |
| Unique reflections ( $R_{\text{int}}$ )          | 185 (0.03)   |
| Unique reflections $F > 4\sigma(F)$              | 178  |
| Structure refinement                             |  |
| Refinement method                                | Full-matrix least-squares on $F^2$                       |
| Weighting coefficients $a, b^*$                  | 0.08260, 28.07100  |
| Data/restraints/parameters                       | 185/0/21   |
| $R_1 [F > 4\sigma(F)]$ , $wR_2 [F > 4\sigma(F)]$ | 0.0516, 0.0527   |
| $R_2$ all, $wR_2$ all                            | 0.1517, 0.1524   |
| Gof on $F^2$                                     | 1.221  |

$P6_3/mmc$  (Table 3). The structural data for the natural analogue of  $\text{NaPb}_2(\text{CO}_3)_2(\text{OH})$ , the mineral abellaite, were obtained by X-ray powder diffraction using the initial model taken from Krivovichev & Burns (2000a). With regard to the ambiguities in the space group assignment and the structure refinement, structural studies of Pb oxysalt minerals and related synthetic compounds are in general challenging due to a number of adverse facts, including strong X-ray absorption by heavy  $\text{Pb}^{2+}$  cations with diffuse electron shells, and marked pseudosymmetries. Atom coordinates and thermal displacement parameters for grootfonteinite are given in Table 6; selected interatomic distances in Table 7.

## 4. Discussion

### 4.1. Cation coordination

The structure of grootfonteinite as described in space group  $P6_3/mmc$  contains two symmetrically independent Pb positions (Fig. 3; Table 6). Pb1 on Wyckoff position  $4f$  (site symmetry  $3m$ ) is coordinated by respectively two O1 atoms of three symmetrically equivalent co-planar carbonate anions resulting in six Pb–O1 bonds of about 2.7 Å. These bonds define an equatorial plane which divides the coordination environment around Pb1 into two hemispheres, in one of which there is a short Pb1–O2 bond of about 2.2 Å, whereas the opposite one contains three additional – very weak – Pb1–O1 bonds of about 3.4 Å. The distortion of the  $\text{PbO}_n$  coordination polyhedron around Pb1 is due to the stereochemical activity of the lone electron pair of  $\text{Pb}^{2+}$ , which also explains the significantly different Pb–O bond lengths within this polyhedron. The Pb1 site is fully occupied by Pb.

Table 5. Comparative data of grootfonteinite and related layered natural and synthetic Pb oxo- and hydroxycarbonates.

| Mineral/compound                                      | Grootfonteinite                                  | Hydrocerussite  | Plumbonacrite   | Synthetic Na,Pb-hydroxycarbonate                            | Abellaite   |
|---|--|---|---|---|---|
| Formula   | Pb <sub>3</sub> O(CO <sub>3</sub> ) <sub>2</sub> | Pb <sub>3</sub> (OH) <sub>2</sub> (CO <sub>3</sub> ) <sub>2</sub> | Pb <sub>5</sub> O(OH) <sub>2</sub> (CO <sub>3</sub> ) <sub>3</sub>                                | NaPb <sub>2</sub> (OH)(CO <sub>3</sub> ) <sub>2</sub>       | NaPb <sub>2</sub> (OH)(CO <sub>3</sub> ) <sub>2</sub> |
| Crystal system  | Hexagonal  | Trigonal  | Trigonal  | Hexagonal/trigonal <sup>†</sup>                             | Hexagonal <sup>†</sup>                                |
| Space group   | <i>P6<sub>3</sub>/mmc</i>                        | <i>R-3m</i> **  | <i>P-3c1</i>  | <i>P6<sub>3</sub>mc/P31c</i>                                | <i>P6<sub>3</sub>mc</i> ****                          |
| <i>a</i> , Å  | 5.3028(10)                                       | 5.2475(1)   | 9.0891–9.0921   | 5.268/5.276   | 5.254(2)  |
| <i>c</i> , Å  | 13.7705(25)                                      | 23.6795(7)  | 24.832–24.923   | 13.474/13.48  | 13.450(5)   |
| <i>V</i> , Å <sup>3</sup>                             | 335.34(1)  | 564.69(1)   | 1776.6–1784.3   | 324.1/324.8   | 321.5(2)  |
| <i>Z</i>  | 2  | 3   | 6   | 2   | 2   |
| <i>R</i> <sub>1</sub> (%)                             | 5.16   | 2.10  | 4.90  | 2.46/4.48   | –   |
| Strong lines of the powder X-ray diffraction pattern: | 4.586(25)  | 4.470 (33)  | 4.26 (80)   | 6.737/6.740 (21/54)*  | 3.193 (100)   |
| <i>d</i> , Å ( <i>I</i> , %)                          | 3.244 (100)                                      | 4.237 (32)  | 3.357 (70)  | 4.327/4.321 (45/40)*  | 2.627 (84)  |
|   | 2.652 (30)                                       | 3.601 (63)  | 2.953 (40)  | 3.369/3.370 (14/59)*  | 2.275 (29)  |
|   | 2.628 (12)                                       | 3.279 (100)   | 2.619 (100)   | 3.203/3.201 (100/100)*                                      | 2.243 (65)  |
|   | 2.294 (21)                                       | 2.632 (88)  | 2.235 (40)  | 2.638/2.634 (45/59)*  | 2.029 (95)  |
|   | 2.054 (39)                                       | 2.230 (23)  | 1.699 (50)  | 2.036/2.034 (41/84)*  | 2.011 (25)  |
| <i>D</i> , g·cm <sup>-3</sup>                         | 6.856 (calc.)                                    | 6.80–6.82 (meas.)***  | 7.07 (meas.)  | 5.86–5.877 (calc.)  | 5.90 (calc.)  |
| Sources   | This work  | *** Palache <i>et al.</i> , 1951; Anthony <i>et al.</i> , 2003    | Palache <i>et al.</i> , 1951; Olby, 1966; Krivovichev & Burns, 2000b; Rumsey <i>et al.</i> , 2012 | Krivovichev & Burns, 2000a; Belokoneva <i>et al.</i> , 2002 | Ibáñez-Insa <i>et al.</i> , 2017                      |

\* Calculated values;

\*\* Unpublished experimental powder X-ray data for hydrocerussite from Merehead quarry, England;

\*\*\* Palache *et al.* (1951) and Anthony *et al.* (2003) do not provide structural data;

\*\*\*\* powder X-ray data indexed after the structural data provided in Krivovichev &amp; Burns (2000a).

† Correct space group is most likely *P6<sub>3</sub>/mmc*.

Table 6. Coordinates and displacement parameters (Å) of atoms in grootfonteinite.

| Atom | Wyck. site  | <i>x</i>  | <i>y</i>   | <i>z</i>    | <i>U</i> <sub>eq</sub> | <i>U</i> <sub>11</sub> | <i>U</i> <sub>22</sub> | <i>U</i> <sub>33</sub> | <i>U</i> <sub>23</sub> | <i>U</i> <sub>13</sub> | <i>U</i> <sub>12</sub> |
|------|-------------|-----------|------------|-------------|------------------------|------------------------|------------------------|------------------------|------------------------|------------------------|------------------------|
| Pb1  | 4 <i>f</i>  | 2/3       | 1/3        | 0.09017(11) | 0.0192(9)              | 0.0186(9)              | 0.0186(9)              | 0.0204(11)             | 0                      | 0                      | 0.0093(5)              |
| Pb2* | 6 <i>h</i>  | 0.2866(7) | −0.2866(7) | 1/4         | 0.020(2)               | 0.025(3)               | 0.025(3)               | 0.011(2)               | 0                      | 0                      | 0.013(2)               |
| O1   | 12 <i>k</i> | 0.141(2)  | 0.281(4)   | 0.1169(19)  | 0.038(5)               | 0.013(6)               | 0.011(9)               | 0.089(15)              | −0.010(10)             | −0.005(5)              | 0.005(4)               |
| O2   | 2 <i>d</i>  | 2/3       | 1/3        | 1/4         | 0.12(5)                | 0.15(7)                | 0.15(7)                | 0.06(5)                | 0                      | 0                      | 0.07(4)                |
| C    | 4 <i>e</i>  | 0         | 0          | 0.122(4)    | 0.037(12)              | 0.031(15)              | 0.031(15)              | 0.05(3)                | 0                      | 0                      | 0.015(8)               |

\* S.O.F. = 0.216(6).

Table 7. Selected bond distances (Å) in the structure of grootfonteinite.

|          |               |             |               |
|----------|---------------|-------------|---------------|
| Pb(1)–O2 | 2.2010(16)    | Pb(2)–Pb(2) | 0.7435(1) × 2 |
| Pb(1)–O1 | 2.687(4) × 6  | Pb(2)–O1    | 2.27(2) × 2   |
| Pb(1)–O1 | 3.356(3) × 3  | Pb(2)–O1    | 2.73(2) × 4   |
| C–O1     | 1.294(19) × 3 | Pb(2)–O2    | 2.87(2) × 2   |

The Pb2 position has been refined as a split atom model on Wyckoff position 6*h* (site symmetry *mm2*). It is thus disordered over three neighbouring positions with unrealistic Pb–Pb distances of about 0.74 Å. The occupancy of this site is significantly less than 1/3 with refined site occupancy of 0.216(6) for Pb. The deviation from 1/3 indicates the presence of minor amounts of Na in accordance with the results of the microprobe analysis (Table 1). An attempt to refine coupled occupancy of Pb

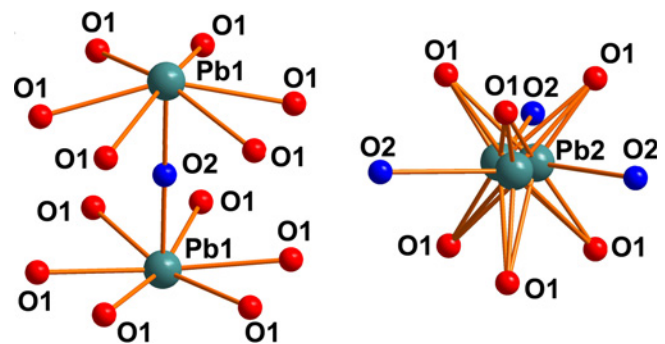


Fig. 3. Coordination environments of Pb1 and Pb2 sites in the structure of grootfonteinite (only strong bonds with lengths &lt; 3.1 Å are shown).

and Na on this site was not successful. In order to maintain charge balance, substitution of Na<sup>+</sup> for Pb<sup>2+</sup> requires some compensation, which we hypothesize to be

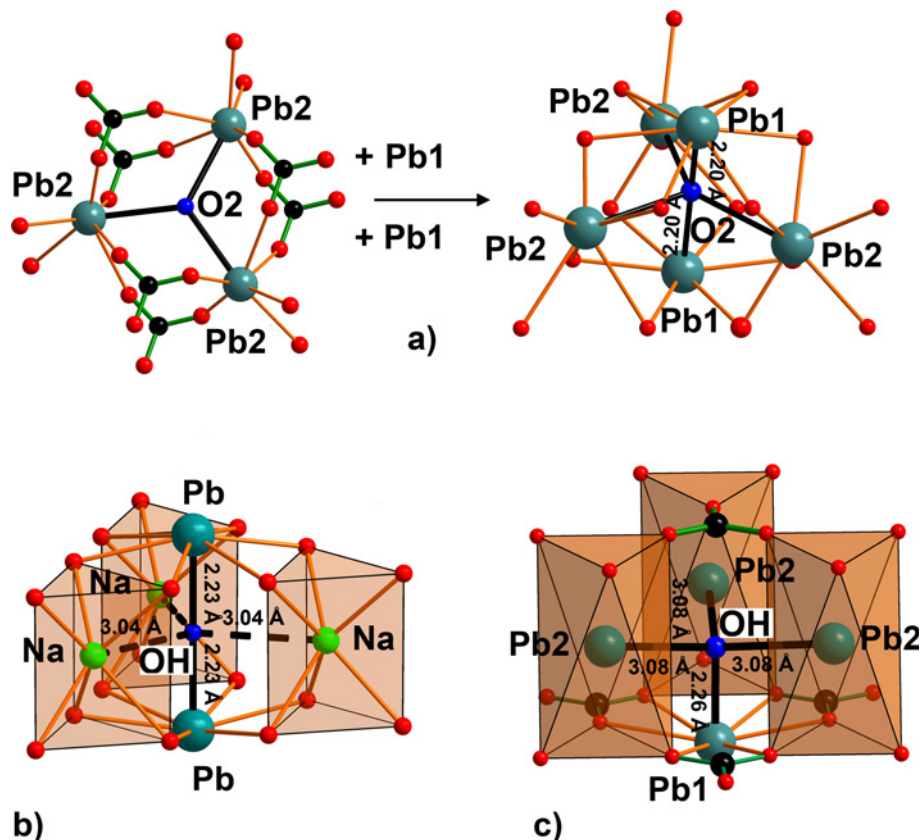


Fig. 4. Coordination environments of the O2 site in the structure of grootfonteinite (a), of the OH site in abellaite (b) and of hydrocerussite (c). For the sake of clarity the disordered Pb2 sites in grootfonteinite and in hydrocerussite are shown as fully ordered. The O2 atom forms three Pb–O bonds in plane, complemented by two strong Pb–O bonds of 2.20 Å with Pb1 atoms in [PbCO<sub>3</sub>]<sup>0</sup> sheets in grootfonteinite (a). The very weak Na–O bonds in abellaite are shown by dashed lines (b). Only one strong Pb–O bond is formed in the crystal structure of hydrocerussite (c).

OH<sup>−</sup> → O<sup>2−</sup> on the O2 site (Fig. 4a). This hypothesis is corroborated by the large value of the refined a.d.p. of O2 which indicates some sort of disorder on this site.

The coordination sphere around the group of disordered and partially occupied Pb2 is symmetrical, with nine oxygens (six O1, three O2) forming a tricapped trigonal prism (Fig. 3, Table 7). This highly symmetrical environment can be considered as the reason to be the reason why the closed-shell Na<sup>+</sup> cation prefers the Pb2 site over the asymmetric Pb1 site.

The crystal structures of both abellaite and synthetic NaPb<sub>2</sub>(CO<sub>3</sub>)<sub>2</sub>(OH) have been reported to contain one symmetrically independent Na and Pb site. The coordination environment of the Pb site corresponds closely to that of the Pb1 site in grootfonteinite, whereas Na takes the place of Pb2. However, unlike the disordered and with respect to Pb under-occupied Pb2 site in grootfonteinite, the Na site in abellaite-type phases is fully occupied and ordered. It is coordinated by six O atoms in a trigonal prismatic arrangement (Fig. 4b), similar to the Pb2 coordination in grootfonteinite (Fig. 3). However, in grootfonteinite the Pb(2)–O(2) bonds (Table 7) in the equatorial plane of the coordination sphere must be taken into account for bond valence calculation, whereas in the Na-bearing phases the corresponding long Na–OH distances can be neglected, as

they do not contribute significantly to the charge saturation of the Na<sup>+</sup> cations. The bond valence sum on the O2 atom of grootfonteinite is considerably higher than that on the OH site in abellaite phases, which suggests a high content of oxygen in this site in grootfonteinite at the expense of OH. However, as a caveat it should be noted that the bond-valence sum on this site cannot be calculated precisely because of the disordered Pb2 site.

The triangular carbonate anions have rather typical values for the C–O bond lengths of 1.294(19) Å.

#### 4.2. General structure description and comparative crystal chemistry

In the structure of grootfonteinite Pb1- and Pb2-centered polyhedra share common O atoms to form 2D (two-dimensional) blocks perpendicular to the *c* axis (Fig. 5a). Notionally, these blocks can be decomposed into three separate sheets (Fig. 6). The two outside sheets contain the Pb1 atoms and CO<sub>3</sub> groups in a 1:1 ratio, are fully ordered and electroneutral giving [PbCO<sub>3</sub>]<sup>0</sup> (Figs. 5a and 6). For the sake of discussion these sheets will be given the generic designation *C*, whereby the symbol refers to the mineral cerussite, PbCO<sub>3</sub>, in the crystal structure of which such sheets occur. Additionally, sheets of composition

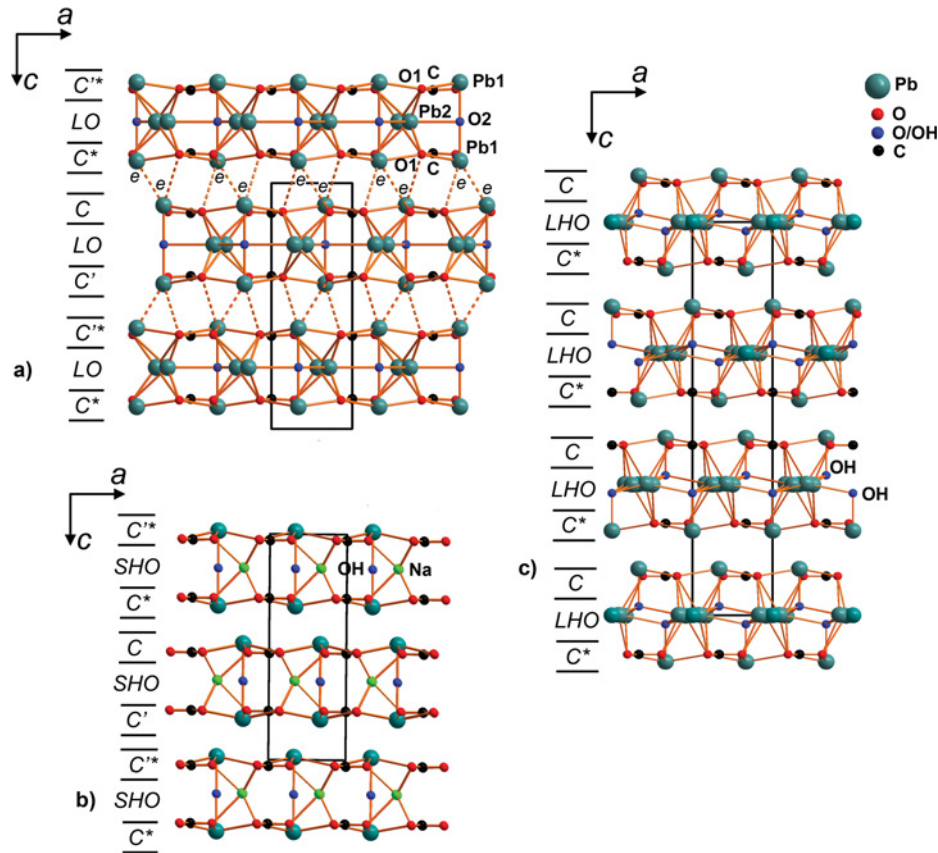


Fig. 5. General projections of the crystal structures of grootfonteinite (a), abellaite (after Ibáñez-Insa *et al.*, 2017) (b) and hydrocerussite from Merehead (based on our unpublished single-crystal X-ray data) (c). 2D blocks can be split into ...*C-LO-C'*..., ...*C-SHO-C'*... and ...*C-LHO-C\**... stackings in the structures of grootfonteinite, abellaite and hydrocerussite, respectively. See the text for details. The possible locations of lone pairs on  $\text{Pb}^{2+}$  cations are symbolized by *e* in the structure of grootfonteinite (a). Similar locations are suggested in between 2D blocks in abellaite and hydrocerussite.

$\{(\text{Pb}_{0.7}\text{Na}_{0.3})[\text{O}_{0.7}(\text{OH})_{0.3}]\}^0$  formed by the Pb2 and O2 sites are sandwiched between every other pair of *C*-type sheets. We denote these sheets as *LO* (*LO*=lead oxide, according to their approximate  $\text{PbO}$  composition). As mentioned before, the presence of minor OH in the O2 site plays the role of a charge-compensating agent for the partial substitution of  $\text{Pb}^{2+}$  by  $\text{Na}^+$ . The formula of the *LO* sheets agrees well with the results of the electron microprobe analysis. In particular, the amount of hydrogen which is calculated from the directly measured contents of metals and oxygen, 0.345 *apfu*, is close to the value obtained from the structure refinement data. The structural formula of the resulting 2D block can be written as  $\{[\text{Pb}(\text{CO}_3)][(\text{Pb}_{0.7}\text{Na}_{0.3})(\text{O}_{0.7}(\text{OH})_{0.3})][\text{Pb}(\text{CO}_3)]\}^0$ . The stereochemically active  $6s^2$  lone electron pairs of the Pb1 atoms are located in between the blocks (Fig. 5a), thus resembling the situation in the structure of litharge, tetragonal  $\text{PbO}$  (Pyykö, 1997). Weak Pb1–O bonds > 3.1 Å provide the 3D connectivity of the crystal structure in grootfonteinite.

The stacking of the sheets can be symbolized as ...*C-LO-C'*..., whereby the primed symbol indicates that the *C* sheets within a given ...*C-LO-C'*... block are related by reflection across a plane perpendicular to [001]. Adjacent *C*

sheets of neighbouring ...*C-LO-C'*... blocks are related by inversion, and this relationship is indicated by a star symbol:  $C \rightarrow C^*$ , or  $C' \rightarrow C'^*$ , respectively. Each of these *C*-type sheets has layer symmetry close to  $p-6m2$  with small deviation from the idealized symmetry. Likewise the indicated symmetry relationships between neighbouring *C* sheets are idealized and do not necessarily correspond to the actual space group symmetry. Thus, the *C* sheets in the structure of grootfonteinite form the following sequence along [001]: ...*C - C' - C^\* - C^\* - C*..., resulting in a periodicity of four sheets distributed over two ...*C-LO-C'*... blocks.

In a similar way, the stacking of the sheets in a given block of abellaite and analogous synthetic  $\text{NaPb}_2(\text{CO}_3)_2(\text{OH})$  is described as ... $[\text{PbCO}_3]$ - $[\text{NaOH}]$ - $[\text{PbCO}_3]$ -... or ...*C-SHO-C'*... (*SHO*=sodium hydroxide) (Fig. 5b, 6), and the overall sequence of the sheets is the same as in grootfonteinite, *i.e.* ...*C - C' - C^\* - C^\* - C*...

The sequence of sheets within a given block of hydrocerussite (Fig. 5c, 6) is ... $[\text{PbCO}_3]$ - $[\text{Pb}(\text{OH})_2]$ - $[\text{PbCO}_3]$ -... or ...*C-LHO-C\**... (*LHO*=lead hydroxide). As in grootfonteinite *C\** denotes a *cerussite*-type sheet which is the inversion image of a *C*-sheet. The *C* and *C\** sheets strictly alternate along [001], and the action of space

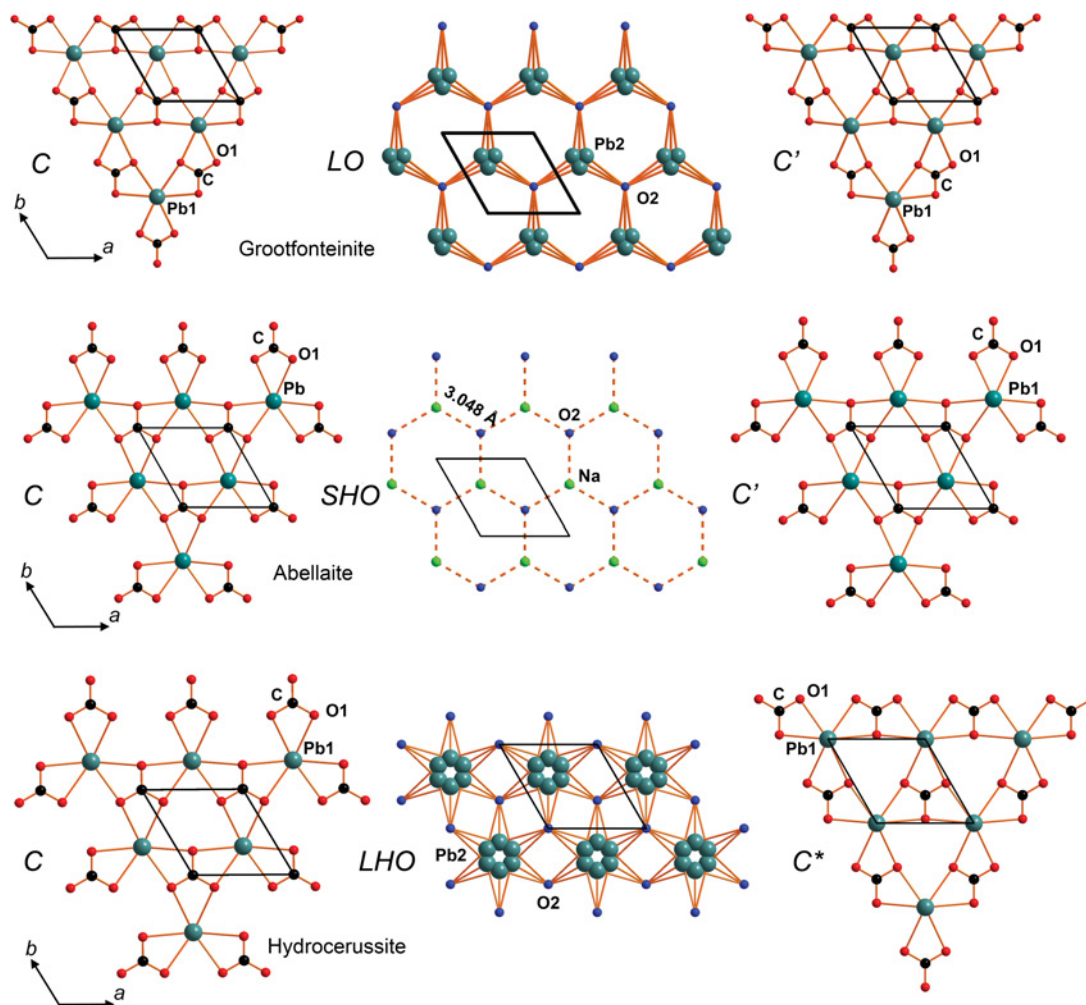


Fig. 6.  $[\text{PbCO}_3]$  (denoted  $C$ ),  $[\text{PbO}]$  (denoted  $LO$ ),  $[\text{NaOH}]$  (denoted  $SHO$ ) and  $[\text{Pb}(\text{OH})_2]$  (denoted  $LHO$ ) sheets forming  $2D$  blocks in the structures of grootfonteinite, abellaite and hydrocerussite.

group  $R-3m$  results in neighbouring blocks shifted by  $(1/3, 2/3, 2/3)$ , in accordance with the  $R$ -centering. Thus, all the blocks are translationally equivalent. The interleaved  $[\text{Pb}(\text{OH})_2]^0$  or  $LHO$  sheets are formed by  $\text{Pb}2$ -like sites with an occupancy factor of  $1/6$ , and the sites which correspond to the  $\text{O}2$  sites in grootfonteinite are fully occupied by  $\text{OH}^-$ . The  $\text{Pb}2$  site (Fig. 4c) forms  $\text{PbO}_6$  polyhedra similar to those around  $\text{Pb}1$  in grootfonteinite or around  $\text{Na}$  in abellaite. In hydrocerussite the  $\text{OH}$  group has one neighboring  $\text{Pb}$  cation underneath or above and one  $C$  atom at a distance of  $3.23 \text{ \AA}$ . This differentiates the  $LHO$  sheets in hydrocerussite structurally from the  $LO$  sheets in grootfonteinite.

Thus, grootfonteinite, abellaite/  $\text{NaPb}_2(\text{CO}_3)_2(\text{OH})$  and hydrocerussite are all composed of layered blocks three-sheet wide, whereby the outside  $[\text{PbCO}_3]$  or  $C$ -sheets are common to all three phases, albeit with possibly different symmetry relationships. The middle sheets,  $LO$ ,  $LHO$  and  $SHO$ , are different. These phases can be considered to constitute a family of merotypic structures (Ferraris *et al.*, 2004). It is possible to conceive other members of this

family by keeping the  $C$  sheets, but changing the middle sheets, and possibly also changing the symmetry relationships between the  $C$  sheets.

Plumbonacrite,  $\text{Pb}_5\text{O}(\text{OH})_2(\text{CO}_3)_3$  (Rumsey *et al.*, 2012) is similar to grootfonteinite in that it also contains an oxo-component, which is represented by additional oxygen atoms (Krivovichev *et al.*, 2013). As in grootfonteinite,  $C$ -type sheets arranged in blocks can be identified. However, their stacking and mutual arrangement is more complicated and the interlayers are far more complex than in grootfonteinite. Thus, in a strict sense plumbonacrite does not belong to the above-mentioned merotype family, and a broader notation, plesiotype, is more appropriate. A detailed discussion of the situation is beyond the scope of the present report, but planned to be published elsewhere.

Shannonite,  $[\text{Pb}_2\text{O}]\text{CO}_3$ , (Roberts *et al.*, 1995), is the only mineral that has a chemical composition very similar to grootfonteinite. However, it has no direct structural relationship with grootfonteinite or the other layered minerals and synthetic phases described in this report.

Macroscopically, plumbonacrite, hydrocerussite, abellaite and grootfonteinite look very similar, typically forming aggregates of platy, lustrous and colourless crystals. Reliable differentiation requires X-ray diffraction, possibly combined with electron microprobe analysis. The latter is indispensable for the discrimination between abellaite and grootfonteinite.

**Acknowledgements:** The authors are grateful to two anonymous reviewers for valuable comments. This work was supported by St. Petersburg State University through the internal grant 3.38.238.2015 (X-ray and structural investigations) and Russian Science Foundation, grant no. 14-17-00048 (microprobe and IR spectroscopy investigations). Technical support by the X-Ray Diffraction Resource Centre of Saint-Petersburg State University is gratefully acknowledged. The Department of Earth Sciences at the Swedish Museum of Natural History (Stockholm, Sweden), and specifically curator Jörgen Langhof, are thanked for the help with access to study and sample collection material.

## References

- Anthony, J.W., Bideaux, R.A., Bladh, K.W., Nichols, M.C. (2003): Handbook of Mineralogy. V. Borates, Carbonates, Sulfates. Mineral Data Publishing, Tucson.
- Belokoneva, E.L., Al'-Ama, A.G., Dimitrova, O.V., Kurzhkovskaya, V.S., Stefanovich, S. Yu. (2002): Synthesis and crystal structure of new carbonate  $\text{NaPb}_2(\text{CO}_3)_2(\text{OH})$ . *Crystallogr. Rep.*, **47**, 217–222.
- Brooker, M.H., Sunder, S., Taylor, P., Lopata, V.J. (1983): Infrared and Raman spectra and X-ray diffraction studies of solid lead (II) carbonates. *Can. J. Chem.*, **61**, 494–502.
- Bruker-AXS (2014): APEX2. Version 2014.11-0. Madison, Wisconsin, USA.
- Criddle, A.J., Keller, P., Stanley, C.J. Innes, J. (1990): Damaraitite, a new lead oxychloride mineral from the Kombat mine, Namibia (South West Africa). *Mineral. Mag.*, **54**, 593–598.
- Ferraris, G., Makovicky, E., Merlino, S. (2004): Crystallography of Modular Materials. IUCr Monographs on Crystallography. Oxford University Press, Oxford.
- Gonzalez, V., Calligaroa, T., Walleza, G., Evenoa, M., Toussainta, K., Menua, M. (2016): Composition and microstructure of the lead white pigment in Masters paintings using HR Synchrotron XRD. *Microchem. J.*, **125**, 43–49.
- Grossman, R.F. & Lutz, J.T. Jr. (2000): Polymer modifiers and additives. CRC Press, 278p.
- Hawthorne, F.C., Abdu, Y.A., Ball, N.A., Pinch, W.W. (2013): Carlfranciscite,  $\text{Mn}_3(\text{Mn}^{2+}, \text{Mg}, \text{Fe}^{3+}, \text{Al})_{42}(\text{As}^{3+}\text{O}_3)_2(\text{As}^{5+}\text{O}_4)_4[(\text{Si}, \text{As}^{5+})\text{O}_4]_6[(\text{As}^{5+}, \text{Si})\text{O}_4]_2(\text{OH})_{42}$ , a new arsenosilicate mineral from the Kombat mine, Otavi Valley, Namibia. *Am. Mineral.*, **98**, 1693–1696.
- Ibáñez-Insa, J., Elvira, J.J., Llovet, X., Pérez-Cano, J., Oriols, N., Busquets-Masó, M., Hernández, S. (2017): Abellaite,  $\text{NaPb}_2(\text{CO}_3)_2(\text{OH})$ , a new supergene mineral from the Eureka mine, Lleida province, Catalonia, Spain. *Eur. J. Mineral.*, **29**, 915–922.
- Innes, J. & Chaplin, R.C. (1986): Ore bodies of the Kombat mine, South West Africa/Namibia. in “Mineral deposits of southern Africa, Geological Society of South Africa”, C.R. Anheusser & S. Maske, eds., 1789–1805.
- Keller, P. (1977): Hydrocerussit von Tsumeb/Südwestafrika. *Der Aufschluss*, **28**, 413–415.
- Krivovichev, S.V. & Burns, P.C. (2000a): Crystal chemistry of basic lead carbonates. III. Crystal structures of  $\text{Pb}_3\text{O}_2(\text{CO}_3)$  and  $\text{NaPb}_2(\text{CO}_3)_2(\text{OH})$ . *Mineral. Mag.*, **64**, 1077–1087.
- , — (2000b): Crystal chemistry of basic lead carbonates. II. Crystal structure of synthetic ‘plumbonacrite’. *Mineral. Mag.*, **64**, 1069–1075.
- Krivovichev, S.V., Mentré, O., Siidra, O.I., Colmont, M., Filatov, S. K. (2013): Anion-centered tetrahedra in inorganic compounds. *Chem. Rev.*, **113**, 6459–6535.
- Le Page, Y. (1987): Computer derivation of the symmetry elements implied in a structure description. *J. Appl. Crystallogr.*, **20**, 264–269.
- Martinetto, P., Anne, M., Dooryhée, E., Walter, P., Tsoucaris G. (2002): Synthetic hydrocerussite,  $2\text{PbCO}_3\cdot\text{Pb}(\text{OH})_2$ , by X-ray powder diffraction, *Acta Crystallogr.*, C58, i82–i84.
- Nysten, P., Holtstam, D., Jonsson, E. (1999): The Långban minerals. in “Långban. The mines, their minerals, geology and explorers, Raster Förlag and the Swedish Museum of Natural History”, D. Holtstam & J. Langhof, eds., 89–183.
- Olby, J.K. (1966): The basic lead carbonates. *J. Inorg. Nucl. Chem.*, **28**, 2507–2512.
- Palache, C., Berman, H., Frondel, C. (1951): Dana’s System of Mineralogy (7th edition), vol. II.
- Peacor, D.R., Essene, E.J., Rouse, R.C., Dunn, P.J., Nelen, J.A., Grice, J.D., Innes, J., von Knorring, O. (1988a): Holdawayite, a new manganese hydroxyl-carbonate from the Kombat mine, Namibia. *Am. Mineral.*, **73**, 632–636.
- Peacor, D.R., Sarp, H., Dunn, P.J., Innes, J., Nelen, J.A. (1988b): Defernite from the Kombat mine, Namibia: A second occurrence, structure refinement, and crystal chemistry. *Am. Mineral.*, **73**, 888–893.
- Pyykö, P. (1997): Strong closed-shell interactions in inorganic chemistry. *Chem. Rev.*, **97**, 597–636.
- Roberts, A.C., Stirling, J.A.R., Carpenter, G.J.C., Criddle, A.J., Jones, G.C., Birkett, T.C., Birch, W.D. (1995): Shannonite,  $\text{Pb}_2\text{OCO}_3$ , a new mineral from the Grand Reef mine, Graham County, Arizona, USA. *Mineral. Mag.*, **59**, 305–310.
- Rumsey, M.S., Siidra, O.I., Krivovichev, S.V., Spratt, J., Stanley, C. J., Turner, R.W. (2012): IMA (11-G): Plumbonacrite is revalidated. CNMNC Newsletter No. 14, October 2012, page 1288; *Mineral. Mag.*, **76**, 1281–1288.
- Sarp, H. & Peacor, D.R. (1989): Jaffeite, a new hydrated calcium silicate from the Kombat mine, Namibia. *Am. Mineral.*, **74**, 1203–1206.
- Scott, D.A., Dennis, M., Khandekar, N., Keeney, J., Carson, D., Dodd, L.S. (2003): An Egyptian cartonnage of the Graeco-Roman period: Examination and discoveries. *Stud. Conserv.*, **48**, 41–56.
- Spek, A.L. (2003): Single-crystal structure validation with the program PLATON. *J. Appl. Crystallogr.*, **36**, 7–13.
- Welcomme, E., Walter, P., Elslände, E. van, Tsoucaris, G. (2006): Investigation of white pigments used as make-up during the Greco-Roman period. *Appl. Phys. A-Mater.*, **83**, 551–556.

Received 1 April 2017

Modified version received 17 June 2017

Accepted 27 June 2017